ICES Journal of Marine Science

ICES Journal of Marine Science (2017), 74(7), 1893–1905. doi:10.1093/icesjms/fsx008

Contribution to the Symposium: '*6th Zooplankton Production Symposium*'

Original Article

The effect of elevated carbon dioxide on the sinking and swimming of the shelled pteropod *Limacina retroversa*

Alexander J. Bergan[1], Gareth L. Lawson[1,*], Amy E. Maas[1,2], and Zhaohui Aleck Wang[3]

[1]*Biology Department, Woods Hole Oceanographic Institution, Woods Hole, MA, USA*
[2]*Bermuda Institute of Ocean Sciences, St. George's GE01, Bermuda*
[3]*Marine Chemistry and Geochemistry Department, Woods Hole Oceanographic Institution, Woods Hole, MA, USA*

**Corresponding author: tel: +508 289 3713; fax: 508 457 2134; e-mail: glawson@whoi.edu.*

Bergan, A. J., Lawson, G. L., Maas, A. E. and Wang, Z. A. 2017. The effect of elevated carbon dioxide on the sinking and swimming of the shelled pteropod *Limacina retroversa*. – ICES Journal of Marine Science, 74: 1893–1905.

Received 22 August 2016; revised 5 January 2017; accepted 11 January 2017; advance access publication 31 March 2017.

Shelled pteropods are planktonic molluscs that may be affected by ocean acidification. *Limacina retroversa* from the Gulf of Maine were used to investigate the impact of elevated carbon dioxide (CO_2) on shell condition as well as swimming and sinking behaviours. *Limacina retroversa* were maintained at either ambient (ca. 400 μatm) or two levels of elevated CO_2 (800 and 1200 μatm) for up to 4 weeks, and then examined for changes in shell transparency, sinking speed, and swimming behaviour assessed through a variety of metrics (e.g. speed, path tortuosity, and wing beat frequency). After exposures to elevated CO_2 for as little as 4 d, the pteropod shells were significantly darker and more opaque in the elevated CO_2 treatments. Sinking speeds were significantly slower for pteropods exposed to medium and high CO_2 in comparison to the ambient treatment. Swimming behaviour showed less clear patterns of response to treatment and duration of exposure, but overall, swimming did not appear to be hindered under elevated CO_2. Sinking is used by *L. retroversa* for predator evasion, and altered speeds and increased visibility could increase the susceptibility of pteropods to predation.

Keywords: locomotion, ocean acidification, shell condition, thecosome pteropod.

Introduction

The chemistry of the oceans is rapidly changing due to the infiltration of anthropogenic carbon dioxide (CO_2) into the surface ocean, a process known as ocean acidification. One of the effects of ocean acidification is a decrease in the availability of carbonate ion (CO_3^{2-}) which affects calcifying organisms that use calcium carbonate ($CaCO_3$) to build shells and other structures (Orr *et al.*, 2005; Raven *et al.*, 2005). A shifting balance of dissolution and calcification as saturation state decreases due to ocean acidification jeopardizes the shell structure that, in many cases, provides protection from predators (Fabry *et al.*, 2008). Ocean acidification could also change the way that some organisms move in their environment because calcified structures govern the movements of certain planktonic organisms, including echinoderms and molluscs (Chan *et al.*, 2011; Wheeler *et al.*, 2013).

Thecosomes, or shelled pteropods (Order Euthecosomata; henceforth referred to simply as pteropods), are planktonic molluscs that build calcium carbonate shells in the crystal form of aragonite, which is less stable than the other common form, calcite. Pteropod shells are becoming increasingly soluble in some regions of their habitat due to ocean acidification (Fabry *et al.*, 2008). The shells of many species of pteropod are transparent, but turn darker and more opaque when exposed to seawater under-saturated with respect to aragonite, possibly due to an increased roughness of the shell's surface associated with partial dissolution (Almogi-Labin *et al.*, 1986; Haddad and Droxler, 1996; Lischka *et al.*, 2011; Lischka and Riebesell, 2012; Wall-Palmer *et al.*, 2013). Laboratory experiments have also shown that lowering the saturation state decreased calcification, leading to impaired shell growth (Comeau *et al.*, 2009, 2010; Bednaršek *et al.*, 2014). Wild caught *Limacina helicina* from regions naturally low in aragonite saturation state have also shown signs of dissolution under scanning electron microscopy (Bednaršek *et al.*, 2012, 2014; Bednaršek and Ohman, 2015).

Shelled pteropods are a food source for many marine organisms, including seabirds, whales, salmon, trout, mackerel, cod, myctophids, and other zooplankton (LeBrasseur, 1966; Ackman *et al.*, 1972; Conover and Lalli, 1974; Levasseur *et al.*, 1994; Pakhomov *et al.*, 1996; Armstrong *et al.*, 2005; Hunt *et al.*, 2008; Karnovsky *et al.*, 2008; Pomerleau *et al.*, 2012; Sturdevant *et al.*, 2013), and hence any effects of ocean acidification on pteropod populations also could have effects on a wide range of marine species. The ability of pteropods to move through the water column could be affected by ocean acidification via changes to the shell. Pteropods have evolved wings, or parapodia, to propel themselves through the water. The spiral-shaped pteropod species (Limacinidae) swim in a zig-zag motion, rotating their shell between a power stroke followed by a recovery stroke to provide lift (Chang and Yen, 2012; Murphy *et al.*, 2016). Many species of pteropods make daily migrations to depth during the day to avoid visual predators and to the surface at night to feed (Wormuth, 1981; Comeau *et al.*, 2012; Maas *et al.*, 2012); sinking of the negatively buoyant shell is presumed to be an important component of the downward part of this diel vertical migration. Pteropods can also use swimming and sinking to escape from predators that are in their immediate proximity (Comeau *et al.*, 2012). Gilmer and Harbison (1986) observed both swimming and sinking behaviours when pteropods were disturbed. Furthermore, after pteropods die, their sinking shells sequester inorganic carbon to the deep ocean (Byrne *et al.*, 1984) and pteropod shells are estimated to account for 12% of the global carbonate flux (Berner and Honjo, 1981). Changes in the fitness, abundance, and sinking of pteropods under ocean acidification thus also have consequences to the carbon cycle.

The species examined in this study, *Limacina retroversa*, is found in the Gulf of Maine, a region that is particularly susceptible to ocean acidification (Wang *et al.*, 2013). Due to deep water formation in the North Atlantic, the infiltration of anthropogenic CO_2 into intermediate and deep water is pronounced in this region and is causing the carbonate chemistry throughout the water column to change more quickly than the average global rate (Sabine *et al.*, 2004). Furthermore, recent studies along the length of the U.S. East Coast found that the Gulf of Maine had the lowest saturation states observed as well as the lowest total alkalinity to dissolved inorganic carbon ratio, indicative of strong sensitivity to continued acidification (Wang *et al.*, 2013; Wanninkhof *et al.*, 2015). Although found year round in the Gulf of Maine, *L. retroversa* is also found in the open ocean, in the temperate and subpolar Atlantic of the Northern and Southern hemispheres. As a broadly distributed species that is also readily available relatively close to shore, it serves as a useful model species for examining the response of pteropods to ocean acidification.

In this study, *L. retroversa* were captured and reared under different concentrations of CO_2 over the course of multiple seasons to examine the impacts on shell condition and locomotion, testing the hypotheses that (i) the appearance of shells changes after exposure to elevated levels of CO_2; (ii) *L. retroversa* sinking speed differs among CO_2 treatments; and (iii) the swimming ability of *L. retroversa* is affected by exposure to elevated CO_2.

Methods

Four cruises into the Gulf of Maine allowed for the capture of shelled pteropods, *Limacina retroversa*. The pteropods were brought back to the laboratory and reared in seawater modified by bubbling with three different levels of CO_2, an ambient treatment (nominally 400 ppm) and two elevated treatments, 800 and 1200 ppm, hereafter referred to as the ambient, medium, and high CO_2 treatments, respectively. These were intended to yield over-saturated, marginal, and strongly under-saturated conditions with respect to aragonite. The actual pCO_2 levels and saturation states achieved via bubbling were calculated from measured dissolved inorganic carbon (DIC) and total alkalinity (TA) using CO2SYS (see below). The condition of shells along with swimming performance and sinking rates of animals were examined after 2 d to 4 weeks of exposure.

Animal sampling

Limacina retroversa were collected in water depths of ca. 45–260 m in the Gulf of Maine near Provincetown, MA aboard the R/V *Tioga* during four cruises in April, August, and November 2014 and April 2015, with each expedition lasting 1–3 d. Oblique tows were conducted with a 1-m diameter Reeve net with 333 μm mesh size. The net was equipped with a large cod-end and hauled at slow speeds (ca. 5 m/min) to collect animals in healthy condition. *Limacina retroversa* were isolated from the rest of the plankton sample and placed into 1-l jars filled with Gulf of Maine seawater pumped *in situ* from a depth of ca. 30 m and filtered through a 64-μm sieve. The pteropods were kept at densities of ca. 30–40 individuals per litre and maintained in a refrigerator at ca. 8 °C and later in coolers for transfer to the laboratory.

Culturing and experimental set-up

Upon returning to the laboratory, *L. retroversa* were moved with a soft pipette into 13-l carboys with two to three replicate carboys per treatment. The carboys were filled with *in situ* seawater collected during the cruise that had been transferred a day earlier to the laboratory and filtered to 1 μm. For the duration of each experiment, as well as for ca. 8–16 h prior to the addition of animals, each carboy was bubbled continuously using one of the three CO_2 concentrations, ambient (nominally ca. 400 ppm), 800, and 1200 ppm. For the medium and high treatments, the target air-balanced CO_2 gases used for bubbling were achieved by mixing pure CO_2 gas and CO_2-free air using mass-flow controllers. The ambient treatment was not controlled but rather was derived from the CO_2 content of ambient air drawn from outside the building.

The carboys were kept in a cold room at 8 °C at a density of ca. 15 individuals per litre. The pteropods were fed a mixed diet of *Rhodomonas lens* (1500–4000 cells/ml) and *Heterocapsa triquentra* (150–500 cells/ml) with lower concentrations provided over the course of each experiment as the pteropod culture density decreased due to mortality and use for various measurements. Water and pteropods were siphoned out of the carboys every week so that the seawater could be replaced with clean pre-bubbled water (collected *in situ* in the Gulf of Maine and kept after the cruise in a holding tank filtered continuously at 1 μm) and dead pteropods could be separated from the live ones. Additional details on culturing protocols can be found in Thabet *et al.* (2015).

During water changes, samples of the water leaving each carboy and the water entering the carboys were collected in 250 ml borosilicate glass bottles, poisoned with 100 μl saturated mercuric chloride, and then capped with a greased stopper for later analysis of TA and DIC. TA was measured using an Apollo SciTech

alkalinity auto-titrator (AS-ALK2, Apollo SciTech, Newark, DE), an Orion 3 Star pH metre, and a Ross combination pH electrode based on a modified Gran titration method (Wang and Cai, 2004). DIC was analysed with a DIC auto-analyzer (AS-C3, Apollo SciTech, Newark, DE) via acidification and non-dispersive infrared CO_2 detection (LiCOR 7000: Wang and Cai, 2004). The saturation state of aragonite (Ω_A), pCO_2, and pH were calculated from DIC and TA with the CO2SYS software (Pierrot *et al.*, 2006), using constants K_1 and K_2 from Mehrbach *et al.* (1973) refitted by Dickson and Millero (1987), and the $KHSO_4$ dissociation constant from Dickson (1990).

In order to monitor conditions and adjust bubbling rates accordingly between water changes, pH in each carboy was measured every 2–3 d using a USB 4000 spectrometer with an LS-1 light source and a FIA-Z-SMA-PEEK 100-mm flow cell (Ocean Optics, Dunedin, FL), and 2 mM m-Cresol indicator dye (50 µl in 20 ml of sample). The DIC/TA-based calculations of Ω_A and pCO_2 described earlier were used as the primary means of assessing the carbonate chemistry of the experimental treatments, but Ω_A and pCO_2 were also calculated using CO2SYS from measurements of pH along with the nearest measurement of TA in time, as a means of assessing variability between water changes.

Shell condition

Ten live animals were removed from each of the ambient, medium, and high treatments at days 2, 4, 8, and 15 during the April 2015 experiment. They were rinsed in deionized water, weighed wet and dry with a Cahn C-33 microbalance with a precision of 1 µg, then placed in 8.25% hypochlorite bleach for 24–48 h to remove tissue, rinsed in deionized water again, and dried.

Using a light microscope, the empty shells were photographed at 2.5× magnification for transparency, opacity, and length measurements. For transparency, the shell was positioned in a glass petri dish with the aperture facing up and the light coming from below and through the shell. A photograph was taken through the microscope with a 2-ms exposure, and with white balance, contrast, and brightness values conserved across images. Similarly, opacity was measured from images of shells placed with the aperture up with 2-ms exposure, but with the lighting coming from two iridescent lights that illuminated the shell parallel to the camera in order to measure reflected light. The lights were positioned opposite each other to reduce shadows, and ∼10 cm away from the shell's location at the centre of the petri dish.

Images were analysed in MATLAB to calculate transmittance and opacity. For transmittance, the shell was identified against the white background by thresholding the image to black and white. The aperture as well as any holes were manually cropped from the object. The transmittance was calculated as the mean greyscale value (range: 0–255) of the pixels of the shell divided by 255 to get a scale of 0 (black) to 1 (white). The image analysis was similar for opacity, but instead the shell was identified by thresholding the brighter shell from a dark background. For opacity, the mean greyscale value of the shell, after cropping out the aperture and any holes, was calculated on the same scale of 0 (black) to 1 (white), like transmittance.

Videography

Live and active *L. retroversa* (shell lengths ranging from 0.56 to 2.37 mm) were removed from each of the CO_2 treated carboys for filming during the 1st, 2nd, 3rd, and 4th weeks of exposure to the different CO_2 treatments. Due to the length of time needed to make a sufficient number of observations, filming was done over 2–5 d for each week. The exact numbers removed from the treatments for each week as well as which weeks were sampled varied among experiments due to variability in the number of live animals available and needs for companion studies of physiology and gene expression. The removed animals were moved to another cold room at 8 °C, in 1-l jars of filtered seawater at the ambient CO_2 concentration. Videos were recorded with a Photron Fastcam SA3 high-speed camera at 500 frames per second. A triangular prism tank with a mirrored face on the hypotenuse of the isosceles right triangle was used so that both the animal and its orthogonal projection were visible in the field of view and the 3D position and velocity of the pteropod could be recorded (Figure 1a). Illumination was delivered by an LED panel with the light diffusing through a thin plastic sheet. The mirrored tank was filled with filtered seawater with a density between 1024 and 1026 kg/m^3. Density was measured with a digital seawater refractometer (Hanna Instruments, model 96822). Three types of movements were examined: sinking with wings withdrawn, sinking with wings extended, and upward swimming.

Sinking

For quantification of sinking rates, a rigid pipette was attached to a ring stand and placed so that the narrow end was in the water and at the top of the camera's frame (Figure 1b and c). The camera was focused and a ruler used to calibrate distance in the tank. The field of view for sinking trials was 5.7 cm×5.7 cm. Each *L. retroversa* was sucked into a soft pipette and then released into the fixed pipette. The constriction in the fixed pipette caused the animal to slow and then accelerate as it left the fixed pipette and sank through the frame. Individual animals were filmed for three to six repeat sinking trials, which were used to calculate average sinking rates for each experimental animal later used in statistical comparisons among treatments. In April, August, and November of 2014, animals were filmed sinking with their wings extended and also with their wings withdrawn. In April 2015, only animals sinking with wings withdrawn were recorded in order to dedicate more time and generate a larger sample sizes for this behaviour, because by then the difference between wings withdrawn and wings extended during sinking had already been determined.

The videos were analysed in MATLAB by converting the frames to black and white. With the pteropod and its reflection isolated as objects, the length and position of the animal and its reflection were measured. Over successive frames, the difference in position was used to calculate speed. As the animals rotated slightly about the horizontal axis the maximum length of the animal or reflection observed over the course of the video was used to estimate the length of the long axis. Speed vs. time plots were fit with a hyperbolic tangent function, giving an analytical solution for terminal speed. The hyperbolic tangent function solves for sinking velocity for a high Reynolds number regime (Owen and Ryu, 2015). The Reynolds number is a non-dimensional number describing the ratio of inertial to viscous forces and is calculated here as animal length multiplied by the speed of the pteropod divided by the kinematic viscosity of water. Although *L. retroversa* move at low to intermediate Reynolds numbers (ca. 5–50), the hyperbolic tangent function fit the data better than the low Reynolds number solution (negative exponential function).

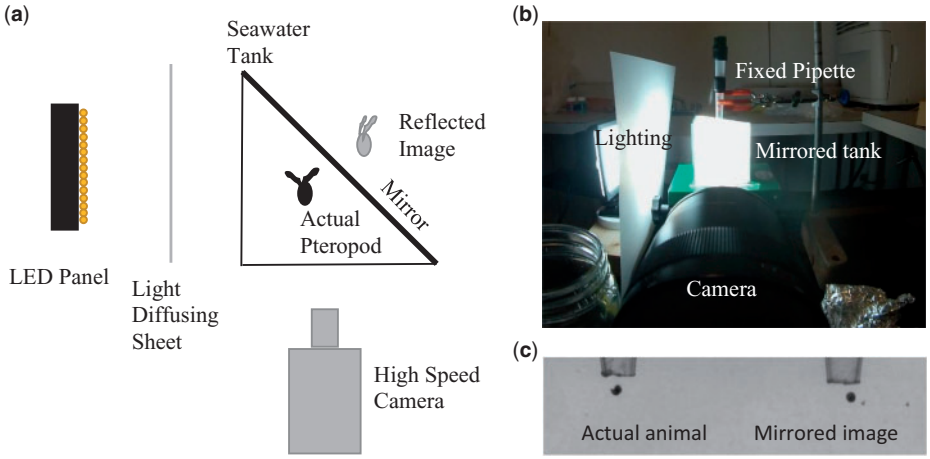

Figure 1. (a) Schematic of the filming set up. The seawater tank had a mirror to show the actual and reflected image of an animal sinking or swimming, allowing position to be determined in three dimensions. A high-speed camera was used for filming and illumination was provided by an LED panel. The tank was 10 cm long, 10 cm wide, and 10 cm high. (b) Filming set up showing the mirrored tank with the fixed pipette that was used to drop the pteropods through for sinking trials. (c) One frame of a video shows the actual image and mirrored image of a sinking pteropod with wings withdrawn, shortly after exiting the fixed pipette.

Swimming

Swimming trials were conducted by placing animals below the camera's field of view via soft pipette and filming their swimming up through the frame. The size of the field of view was calibrated with a ruler and was 2.7 cm×2.7 cm, with the bottom of the field of view 2–3 cm above the floor of the tank. In the April 2014 and August 2014 experiments, multiple pteropods from the same treatment were placed in the tank together and swimming trials were recorded. Each of these swimming trials was included separately in statistical comparisons among treatments, but because the exact identity of swimmers was not known, the more active individuals could have contributed multiple swimming observations. Therefore, for improved accuracy, in November 2014 and April 2015, a single individual was placed in the tank and multiple swimming trials were recorded for each animal; swimming metrics averaged over the multiple trials for each individual were then used in statistical comparisons among treatments.

Video analysis was done in MATLAB with similar protocols as for sinking. The frames were converted to black and white to allow for the identification of the pteropod and its reflection to track its properties (length, position) from one frame to the next. These properties were used to determine the speed, distance travelled, and trajectory. Path tortuosity was measured as the total cumulative distance travelled over a video segment divided by the direct distance between the last and first frame; each video segment was at least 0.5 s and recorded at least three wing beats (power and recovery strokes). The swimming metrics examined were the mean speed (calculated in 3D), frequency of wing beats, path tortuosity, ratio of horizontal to vertical displacement, and asymmetry of speed between the power and recovery strokes (Figure 2).

Statistics

One-way analyses of variance (ANOVA), or a Kruskal–Wallis one-way ANOVA on ranks when the data failed either the equal variance or normality tests, were used to test for differences among treatments in shell transmittance and opacity, sinking speeds (separately for wings withdrawn and extended), swimming speed, wing beat frequency, swimming path tortuosity, ratio of horizontal to vertical displacement, and asymmetry in speed between the power stroke and recovery stroke. If there were significant effects from these tests, *post hoc* pairwise comparison tests were conducted using the Holm–Sidak method for one-way ANOVAs and Dunn's method for Kruskal–Wallis one-way ANOVAs. Sinking speed with wings withdrawn was compared with sinking speed with wings extended using a Wilcoxon Paired-Sample Signed-Rank signed rank test. Correlation coefficients were also calculated among swimming metrics.

Results

Experimental treatments

The nominal target values for pCO_2 of 400, 800, and 1200 µatm were not always achieved and calculated values varied among experiments, but overall the carbonate chemistry measurements indicated clear distinctions among treatments (summarized in Table 1 and see Supplementary Table S1 for full details). The ambient treatment had higher levels than the nominal 400 µatm (the approximate global average atmospheric concentration), closer to 450 µatm. Calculations of achieved pCO_2 for the medium and high treatments also indicated variability, likely due to a combination of uncertainty in the sampling and measurements of DIC and TA, uncertainty in the mixture of gas by the mass-flow controllers, and variability in the degree of bubbling. In April and August 2014, the calculated pCO_2 of pre-bubbled water that was entering the carboys at the onset of the experiment was consistently lower than that calculated for the outgoing water, suggesting incomplete pre-equilibration (Supplementary Table S1). Subsequent measurements of pH made between water changes, however, indicated that the seawater chemistry for these treatments attained their target values after <24 h.

Measurements of outgoing water made during water changes indicated that the ambient treatments always had over-saturated conditions with respect to aragonite (Ω_A=1.49–1.61), medium treatments were near the threshold of saturation (0.76 in November 2014, 1.21 in August 2014, and otherwise 0.94–1.05), and the high treatment had strongly under-saturated conditions

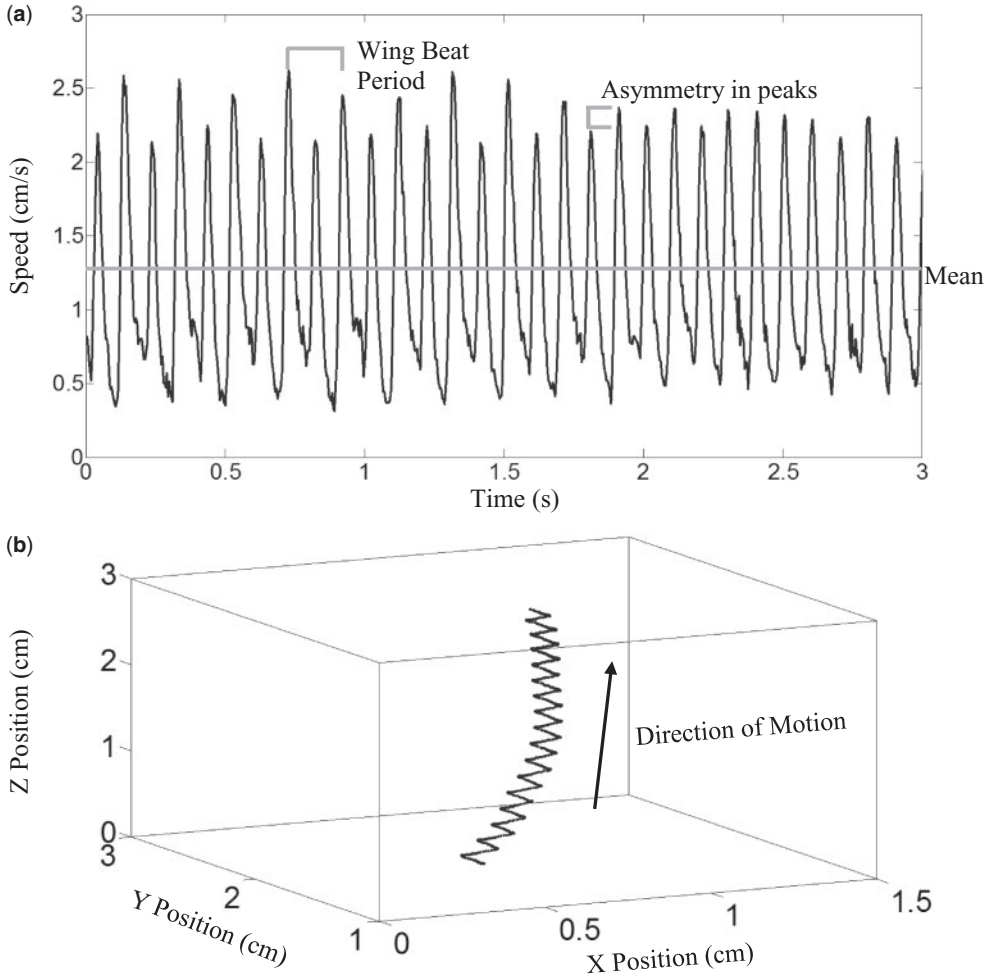

Figure 2. (a) Speed vs. time plot of a swimming trial, showing the full time-series of speed from the 3-s video segment, along with calculated mean speed, a wing beat period, and the asymmetry in peaks. The wing beat frequency was calculated as 1/(beat period) and included both the power and recovery strokes. Power strokes were consistently associated with greater speeds and asymmetry between the peak speeds of the power and recovery stroke was measured as the difference between subsequent peaks of speed divided by the larger of the two. (b) The 3D trajectory of a swimming *L. retroversa* shows the pattern of motion. Note that this is a scatter plot but the high frame rate of the camera leads to the points appearing essentially as a line. Tortuosity was calculated as the total cumulative distance traveled divided by the direct distance from starting point to finish.

(Ω_A=0.63–0.80, Table 1). The medium treatment showed the greatest variability, likely due to a combination of sampling error, issues with the mass-flow controllers (in November 2014, where saturation states were overly low), and insufficient bubbling (in August 2014, where saturation states were overly high). The ambient treatment was significantly different in aragonite saturation state from both of the elevated CO_2 treatments in three of the experiments (one-way ANOVA, $p < 0.001$), while in the August 2014 experiment only the ambient and high treatments were significantly different (Kruskal–Wallis one-way ANOVA, $H = 11.7$, $p = 0.003$). The medium and high treatments were also significantly different from one another in April of 2014 and 2015 (Holm–Sidak, $p < 0.05$), though not in August or November 2014. TA showed relatively small differences between experiments, presumably related to natural seasonal processes in the Gulf of Maine region (Supplementary Table S1).

Shell condition

Shell condition from the April 2015 experiment for the ambient treatment was mostly unchanged relative to duration of exposure, while the medium and high CO_2 treatments showed decreased transmittance and increased opacity over the course of 15 d of exposure (Figure 3 and Table 2). On day 2, there was not a significant difference in the appearance of shells among treatments, but both shell transmittance and opacity were significantly different among treatments on days 4, 8, and 15 (Table 3). *Post hoc* pairwise comparisons showed that the transmittance from the ambient and high treatments were significantly different on days 4, 8, and 15 ($p < 0.05$), the medium and high treatments were never significantly different, and the medium and ambient treatments were only significantly different on day 15 ($p < 0.05$). For opacity, on days 4 and 8, only the ambient and high treatments were significantly different ($p < 0.05$), whereas on day 15, each treatment was significantly different from the others ($p < 0.05$).

Table 1. The carbonate chemistry parameters partial pressure of CO_2 (pCO_2), pH, and aragonite saturation state (Ω_A) are average values for the water leaving the treatment carboys at days 7 and 14 during water changes.

Experiment	Treatment	pCO_2 (μatm)	pH	Ω_A
April 2014	Ambient	470±20	7.96±0.02	1.54±0.06
	Medium	850±40	7.73±0.02	0.94±0.03
	High	1190±120	7.59±0.04	0.70±0.07
Aug 2014	Ambient	440±40	7.98±0.03	1.58±0.11
	Medium	650±170	7.84±0.11	1.21±0.30
	High	990±100	7.66±0.04	0.80±0.08
Nov 2014	Ambient	480±50	7.95±0.04	1.49±0.11
	Medium	1100±290	7.63±0.10	0.76±0.15
	High	1320±160	7.55±0.05	0.63±0.07
April 2015	Ambient	440±30	7.99±0.03	1.61±0.09
	Medium	740±100	7.78±0.05	1.05±0.12
	High	1180±190	7.59±0.07	0.70±0.11

TA and DIC were directly measured and were used for calculation of the other parameters. Measurements of ingoing water at the start of each week of exposure in April and August 2014 appeared to indicate insufficient pre-equilibration, although target levels were reached by day 1 (see text and Supplementary Table S1). The values are reported as the mean ± standard deviation.

The dry masses of the shells (with animal body tissue present) from April 2015, normalized to length, indicated an overall decrease over the course of the 15 d of exposure and also substantial overlap among treatments (Supplementary Figure S1). Mass normalized to length was significantly different between the CO_2 treatments at days 8 (Kruskal–Wallis one-way ANOVA, $H=6.1$, $p=0.048$) and 15 (one-way ANOVA, $F=4.1$, $p=0.037$), but not for the earlier time points. At day 8, there were not significant pairwise differences in mass normalized to length among treatments (Dunn's method, $p>0.05$), and on day 15, only the medium and high treatment were significantly different from one other (Holm–Sidak method, $p<0.05$).

Sinking

Sinking rates showed differences associated with treatment, duration of exposure, experiment, and behaviour (i.e. wings extended or withdrawn). After 1 week of exposure, sinking rates for animals with wings withdrawn were similar among treatments and showed no significant differences for two of three experiments (Figure 4a and Table 3), while during week 1 of the third experiment (April 2015) sinking rates differed significantly among treatments. Sinking rates were significantly slower for animals in the elevated CO_2 treatments than in the ambient treatment after two or more weeks of exposure during every experiment. In all pairwise comparisons, the ambient treatment was significantly different from both the medium and high treatments, except for the second week of the November 2014 when only the ambient and high treatments were significantly different ($p<0.05$).

On an average, there was an 84% reduction in sinking speed for animals holding their wings extended compared with wings withdrawn, and sinking speeds with wings withdrawn and wings extended measured for the same individuals were significantly different (Wilcoxon Paired-Sample Signed Rank, $Z=-8.981$, $p<0.001$). Sinking rates for animals with wings extended also showed similar trends to those with wings withdrawn with respect to treatment and duration of exposure (Figure 4b). While there were no significant differences among the treatments after 1 week of exposure, significant differences were observed among treatments after an exposure duration of 2 weeks and onwards, with significantly faster sinking rates evident for the *L. retroversa* exposed to ambient CO_2 compared with the high treatment (November 2014 week 2) or to the medium and high treatments (April 2014 week 4).

In order to account for possible uncertainty introduced by any differences in the size of animals among treatments and time points, attempts were also made to normalize the sinking rate measurements relative to individual size. Linear regressions based on log–log plots were used to examine the effect of length on sinking speed of animals with wings withdrawn. The resulting power law scaling relationships between sinking speed and length for the ambient, medium, and high treatments were 0.45, 0.74, and 0.52, respectively (Figure 5), suggesting that normalizing the sinking speeds by the square root of length (0.50 scaling) was appropriate. In all but one case, normalizing sinking speed by length in this way did not affect the significance of the differences among treatments, with the exception of week 1 for November 2014. In this case, in contrast to the initial test, when normalized, the Kruskal–Wallis one-way ANOVA showed significant differences among treatments in sinking speeds ($H=7.3$, $p=0.026$) due to faster sinking in the high treatment, followed by the medium, then ambient.

Swimming

In contrast to sinking, swimming rates did not differ in a consistent manner among treatments and durations of exposure. For the two experiments (August 2014 and April 2015) where observations were made after 1 week, mean swimming speed was significantly different among treatments but differed in which treatment showed the fastest swimming (Figure 6a and Table 3). Significant differences were not seen among treatments at 2 or 3 weeks. There was also not a significant correlation between swimming speed and animal length (Table 4): in the log–log plot of swimming speed vs. animal length the slopes of the linear regressions were nearly zero (see Supplementary Figure S2) and hence no attempts were made to normalize swimming measurements to animal size.

For the initial two experiments (April and August 2014) where multiple animals were together in the filming tank and individual swim analyses were not possible, wing beat frequency showed no differences among treatments (Figure 6b and Table 3). For the two later experiments (November 2014 and April 2015), where individual animals were measured separately, a trend of decreasing flapping frequency under elevated CO_2 was evident, and the frequency of wing beats was significantly higher in the ambient treatment compared with the medium and high treatments in week 1 of the April 2015 experiment, although not in week 2 of the November 2014 experiment or week 2 of April 2015.

Tortuosity only differed significantly during the initial experiments (April 2014 and August 2014), where multiple animals were placed together during filming (Figure 6c and Table 3). In the November 2014 and April 2015 experiments, no significant differences were seen in tortuosity among the treatments, although there was a high degree of variability during the November 2014 week 2 experiment, where the ambient treatment had the highest tortuosity due to an outlier (4.05) and low sample

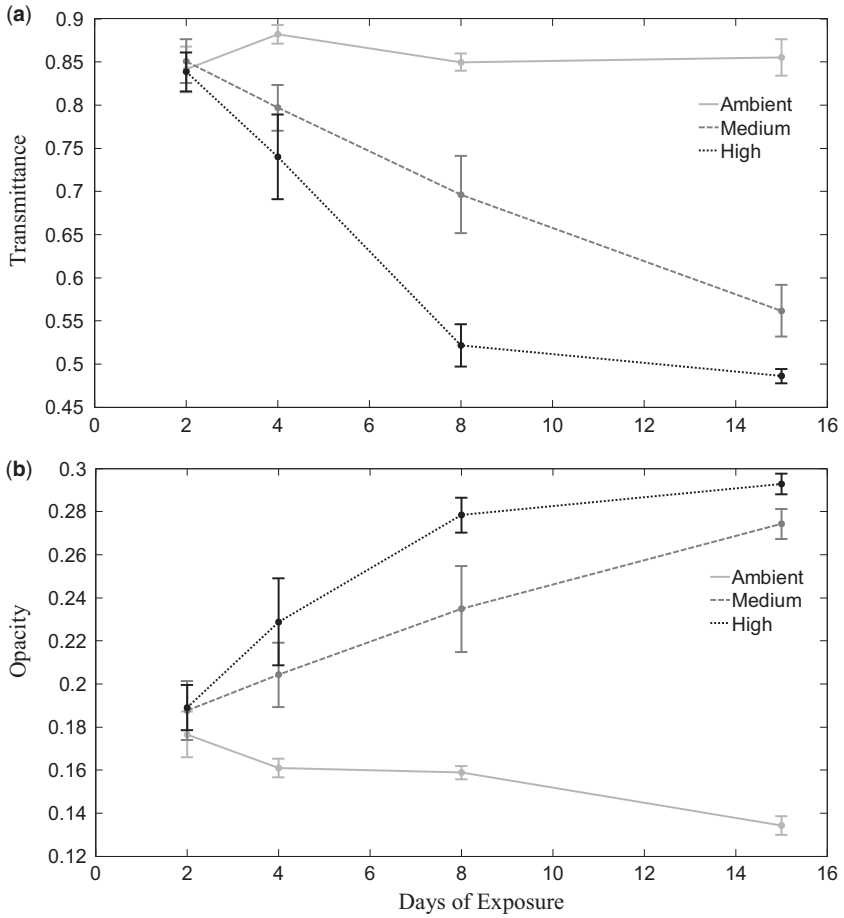

Figure 3. (a) Transmittance (proportion of transmitted light) and (b) opacity (proportion of reflected light) of *L. retroversa* shells from the April 2015 experiment relative to duration of exposure for each of the three CO_2 treatments. Error bars denote standard error.

size (n = 3). The average ratio of horizontal to vertical displacement averaged over all the experiments was 0.35 ± 0.15 (±s.d.) and similar to tortuosity there were only significant differences between treatments in April 2014 (Kruskal–Wallis one-way ANOVA, $H = 8.7$, $p = 0.013$) and August 2014 (Kruskal–Wallis one-way ANOVA, $H = 6.9$, $p = 0.032$). The asymmetry between the peak speeds of the power and recovery strokes did not differ among treatments for any of the experiments (one-way ANOVA). The average and standard deviation of asymmetry between the power/recovery strokes over all the experiments was 7.2 ± 5.1% ($n = 191$).

There was a significant positive correlation between mean swimming speed and wing beat frequency and a significant negative correlation between wing beat frequency and length (Table 4). The mean swimming speed also had significant negative correlations with both tortuosity and the asymmetry between the speeds of the power and recovery strokes. There were no significant correlations between tortuosity or the asymmetry of the strokes and length.

Discussion

The condition of *Limacina retroversa* shells and sinking speeds of live animals were significantly affected by exposure to elevated CO_2. As the passive motion of sinking was slower in the elevated CO_2 treatments, even for animals with wings withdrawn, this indicates that the slower sinking rates likely relate to differences in the shells. Swimming behaviour showed less clear patterns of variability in relation to treatment and duration of exposure, and overall swimming ability did not appear to be hindered under elevated CO_2.

Shell condition

The appearance of shells changed significantly in the elevated CO_2 treatments. Differences in transmittance and opacity of the shells from the medium and high treatments relative to the ambient treatment were apparent from day 4 of exposure, while in contrast the shells from the ambient treatment did not change significantly over time. Other studies have found that short exposures to similar CO_2 concentrations (750, 880, and 1000 ppm for 7–8 d) can cause changes in shell condition of *L. retroversa* (Lischka and Riebesell, 2012; Manno *et al.*, 2012) and in the congeneric species *L. helicina* (Lischka *et al.*, 2011; Bednaršek *et al.*, 2012, 2014; Busch *et al.*, 2014). The present study adds to these earlier observations by offering a new, quantitative metric for assessing shell condition based on transparency to light-based microscopy and by extending the duration over which effects on shell condition were examined. Although they were measured and considered separately, transmittance and opacity are highly related optical properties and as such expectedly showed very similar patterns (though in opposing directions). Future studies

Table 2. Representative images showing the changes in shell appearance from day 2 to day 15 for each treatment during the April 2015 experiment.

Treatment	Day 2	Day 15
Transmittance		
Ambient		
Medium	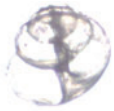	
High	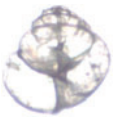	
Opacity		
Ambient	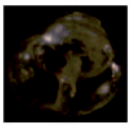	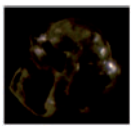
Medium	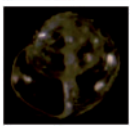	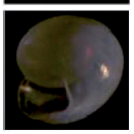
High	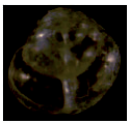	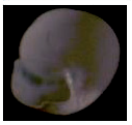

Transmittance images were taken with light shining from below the sample, and opacity images were taken with light illuminating the sample from the sides.

employing our light microscopy-based approach might thus focus on transmittance, because the transverse lighting used for opacity measurements causes some glare on the shells regardless of condition which may affect the sensitivity of this metric.

A loss of transparency could have a negative impact on shelled pteropods because transparency is a form of camouflage in the open ocean environment. Although some pteropod predators, notably the gymnosome (or shell-less) pteropods, are non-visual, the decrease in transparency could potentially serve to increase visibility to visual predators known to feed on pteropods, such as fish and birds (LeBrasseur, 1966; Levasseur *et al.*, 1994; Armstrong *et al.*, 2005; Hunt *et al.*, 2008; Karnovsky *et al.*, 2008; Sturdevant *et al.*, 2013). It is not known how small of a change in CO_2 concentration will elicit a response in shell condition, but it is noteworthy that changes were evident here in the medium treatment, which in April 2015 was just above an aragonite saturation state of one, a potential environmental threshold. The loss of transparency is likely caused by dissolution of the calcium carbonate matrix, as has been seen at higher resolution using scanning electron microscopy (Bednaršek *et al.*, 2012). It is possible that the more gradual change in CO_2 concentrations that will occur as a result of climate change could allow for adaptation, although shell dissolution has already been documented for wild populations of *L. helicina* exposed to naturally low saturation state conditions (Bednaršek *et al.*, 2012, 2014). The methods provided here for examining the transparency of shells could be applied to natural populations to look for seasonal and interannual changes.

Sinking

Although sinking speeds have been previously quantified in some pteropod species (Lalli and Gilmer, 1989), the effect of elevated CO_2 on pteropod sinking has not previously been examined,

Table 3. Cruise and experiment details and associated statistics.

Experiment	Cruise dates	Type of observation	Exposure duration	Sample size (Amb., Med., High)	One-way ANOVA: *F* Kruskal-Wallis one-way ANOVA: *H*
April 2014	25 April–27 April 2014	Sinking	4 weeks	10, 10, 7	Sinking wings in: $F=9.8^{***}$; Sinking wings out: $F=9.0^{**}$
		Swimming	3 weeks	11, 7, 10	Swim speed: $F=0.9^{NS}$, Beat: $H=1.7^{NS}$, Tort: $H=8.4^{*}$
August 2014	19 August 2014	Sinking	1 week	10, 12, 13	Sinking wings in: $H=1.1^{NS}$, Sinking wings out: $F=1.0^{NS}$
		Swimming	1 week	13, 21, 17	Swim speed: $F=4.6^{*}$, Beat: $H=2.1^{NS}$, Tort: $H=10.6^{**}$
November 2014	4 November–6 November 2014	Sinking	1 week	20, 22, 20	Sinking wings in: $F=0.3^{NS}$, Sinking wings out: $F=0.4^{NS}$
		Sinking	2 weeks	25, 20, 18	Sinking wings in: $F=4.2^{*}$, Sinking wings out: $F=6.4^{**}$
		Swimming	2 weeks	3, 10, 10	Speed: $H=1.6^{NS}$, Beat: $F=1.6^{NS}$, Tort: $H=2.3^{NS}$
April 2015	26 April–27 April 2015	Sinking	1 week	25, 26, 25	Sinking wings in: $F=5.8^{**}$
		Sinking	2 weeks	26, 26, 22	Sinking wings in: $H=11.6^{**}$
		Sinking	3 weeks	26, 22, 16	Sinking wings in: $F=19.0^{***}$
		Swimming	1 week	15, 18, 16	Swim speed: $F=3.7^{*}$, Beat: $F=9.5^{***}$, Tort: $H=4.7^{NS}$
		Swimming	2 weeks	8, 14, 18	Swim speed: $F=0.1^{NS}$, Beat: $F=1.5^{NS}$, Tort: $H=5.1^{NS}$
		Shells	2 d	8, 9, 8	Transmittance: $F=0.1^{NS}$, Opacity: $H=0.8^{NS}$
		Shells	4 d	8, 8, 8	Transmittance: $H=9.0^{*}$, Opacity: $H=8.1^{*}$
		Shells	8 d	8, 7, 5	Transmittance: $H=14.5^{***}$, Opacity: $H=13.0^{**}$
		Shells	15 d	7, 7, 5	Transmittance: $F=60^{***}$, Opacity: $F=212^{***}$

For each type of observation of *L. retroversa* (shell condition, sinking, or swimming) and each duration of exposure, the sample sizes are listed (ambient, medium, high). Test statistics (*F* for one-way ANOVAs and *H* for Kruskal–Wallis one-way ANOVAs on ranks) are reported for comparisons among treatments for multiple sinking, swimming, and shell variables abbreviated as follows: "Sinking wings in" is sinking speed with wings withdrawn, "Sinking wings out" is sinking speed with wings extended, "Swim speed" is mean swimming speed, "Beat" is wing beat frequency, and "Tort" is tortuosity.

$^{*}p < 0.05$, $^{**}p < 0.01$, $^{***}p < 0.001$.

NS, non-significant.

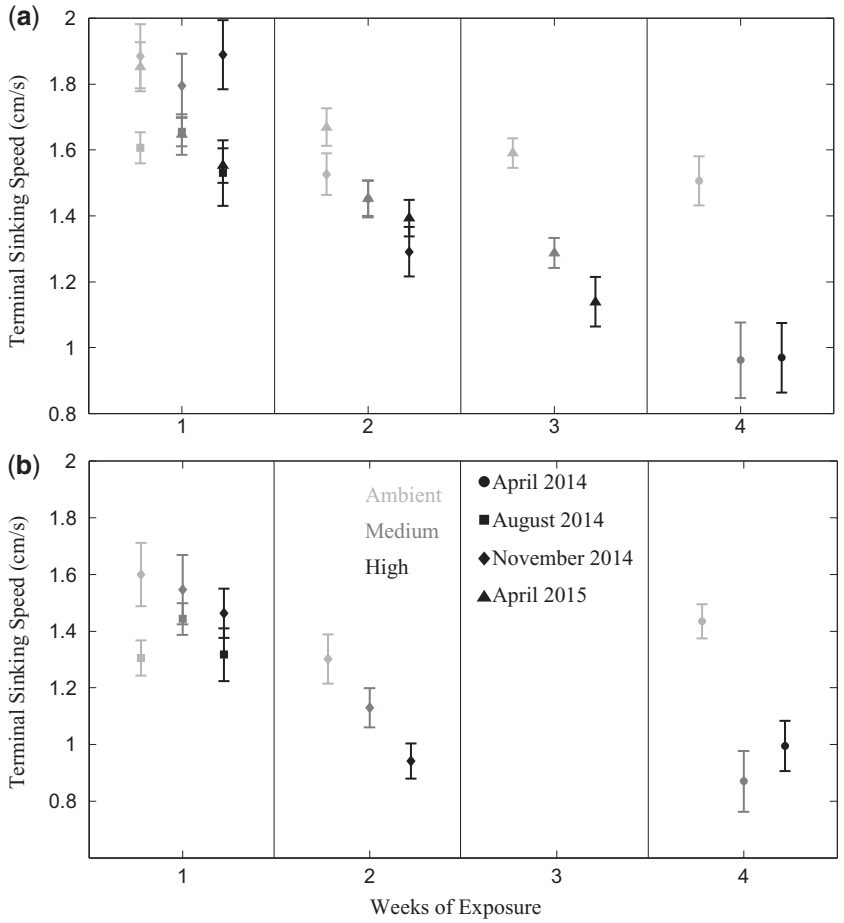

Figure 4. (a) Terminal sinking speed for *L. retroversa* with wings withdrawn for the four experiments (circle: April 2014; square: August 2014; diamond: November 2014; triangle: April 2015) after durations of exposure of 1–4 weeks. From left to right within each weekly bracket the ambient, medium, and high treatment are plotted, although the treatments were measured together over the course of 2–5 d and are spaced along the *x* axis simply for easier visualization. The error bars denote standard error. (b) The terminal sinking speed with wings extended for the April 2014, August 2014, and November 2015 experiments. No measurements of sinking with wings extended were made in April 2015 or in week 3 of any of the experiments.

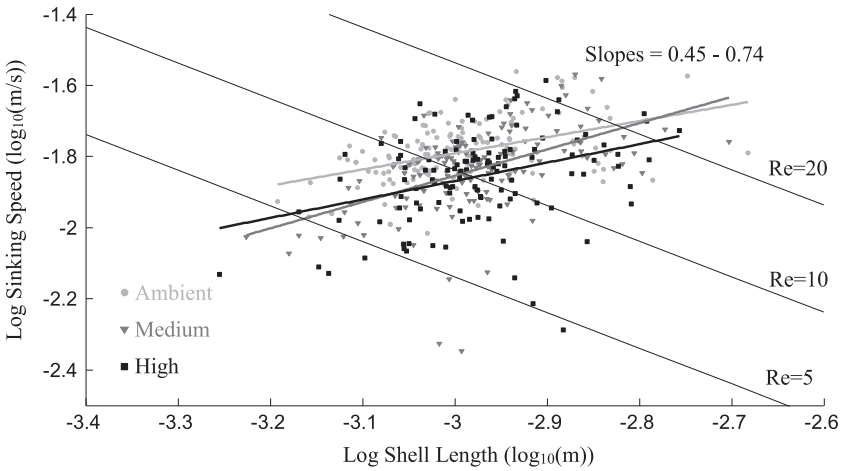

Figure 5. Log_{10} terminal sinking speed with wings withdrawn vs. log_{10} shell length for each treatment (points) along with a linear regression for each treatment (lines). The slope of the linear regressions shows the power scaling between sinking speed and shell length. Contours of constant Reynolds numbers (Re) of 5, 10, and 20 are shown in black.

despite the important role that sinking plays in pteropod locomotion and carbonate flux. In this study, the sinking speeds of *L. retroversa* were slower during the second week of exposure to elevated CO_2 and onwards. Measurements of mass made for the April 2015 experiment, normalized to length to account for variability in size, did not indicate a clear pattern among treatments indicative of dissolution due to exposure to enhanced CO_2. It is thus not clear whether the changes in sinking speed are due to the shells changing in mass, density, or if they are modified in a way that increases drag. It is also not known whether the experimentally manipulated chemical conditions had any impacts on the mass of the animal bodies, separate from the shells. Given the relatively massive shells and direct linkage between undersaturated conditions and calcium carbonate dissolution, however, it seems likely that changes in sinking speed relate primarily to changes in the shells. The ambient treatment also showed slower sinking with increased duration of exposure, but nonetheless the effect of elevated CO_2 treatment was persistent and sinking both with wings withdrawn and extended showed a similar treatment effect. The decrease in sinking speed for the ambient treatment could indicate a captivity effect, where animals in all treatments might decrease in overall health and vigour with increased duration of time in captivity. It could also be due to removal of larger individuals earlier in the experiments, leading to smaller pteropods being tested in the later weeks, although the effect of exposure on sinking speed was consistent when normalized by the square root of length (based on the observed relationship between size and sinking speed) so this is less likely. In an earlier study, the scaling between shell length and sinking speed for the congeneric species *L. helicina* was between 0.3 and 0.4 (Chang and Yen, 2012), similar to the scaling of 0.5 found in this study. Animal length and speed are also important in determining the Reynolds number (Re). As *L. retroversa* moves in a transitional regime of Re between ca. 5 and 50, decreases in sinking and swimming speeds might lead to a decrease in Re that could result in increased viscous drag (Walker, 2002).

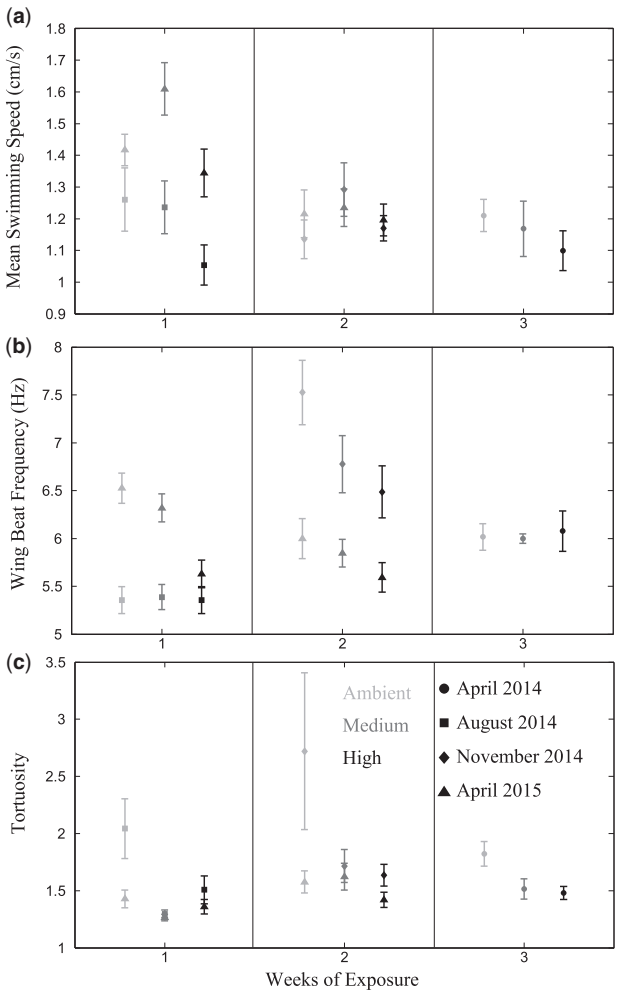

Figure 6. (a) Mean swimming speed, (b) wing beat frequency, and (c) tortuosity for *L. retroversa* for the four experiments (circle: April 2014; square: August 2014; diamond: November 2014; triangle: April 2015) after durations of exposure of 1–3 weeks. From left to right within a week the ambient, medium, and high treatment are plotted, although treatments were measured together over the course of 2–5 d. The error bars denote standard error. Both the power and recovery stroke are included in each wing beat in calculating wing beat frequency.

Extended wings slowed sinking, presumably as an adaptation to minimize energetic expenditure on swimming to maintain position in the water column. In the laboratory, our observation is that pteropods alternate periods of swimming upwards with sinking, while in the field, the production of mucous webs is thought to slow or even halt sinking, although the prevalence of this behaviour is not well known (Gilmer and Harbison, 1986). The bio-energetic consequences to pteropods in the wild of reduced sinking speeds are thus somewhat difficult to assess, but it may be that metabolic costs of maintaining position in the water column are overall reduced under exposure to enhanced CO_2. In contrast, changes in sinking speed may have negative consequences in terms of vulnerability to predation. The gymnosome pteropods feed exclusively on shelled pteropods and for this monospecific predator–prey relationship, withdrawing wings into the shell might make it harder for the predatory shell-less pteropods to successfully capture and consume their prey (Conover and Lalli, 1974). Sinking behaviour in the wild is also believed to

Table 4. Correlation coefficients (r) among the swimming variables: mean swimming speed, wing beat frequency, path tortuosity, and asymmetry between the peaks of speed (i.e. the difference between the power and recovery stroke).

Correlation coefficient	Length	Wing beat frequency	Tortuosity	Asymmetry in peaks
Speed	0.0005^{NS}	**0.2395^{***}**	**-0.4357^{***}**	**-0.18233^{*}**
Length		**-0.3785^{***}**	-0.1418^{NS}	0.110331^{NS}
Wing beat			0.1209^{NS}	-0.13198^{NS}
Tortuosity				0.059909^{NS}

Bold indicates significant correlations.
$^{*}p < 0.05$, $^{**}p < 0.01$, $^{***}p < 0.001$.
NS, non-significant.

be a mode of predator avoidance: a response to a disturbance was noted for the pteropod species *Diacria quadridentata*, which withdrew its wings presumably to achieve a faster sinking speed (Gilmer and Harbison, 1986). Overall, there are only a few field observations of pteropod behaviour in the wild, but along with the decrease in transparency and camouflage, a decrease in sinking speed with increased CO_2 is another way that *L. retroversa* and other shelled pteropods might have increased vulnerability to predators due to ocean acidification.

Post-mortem sinking of pteropod shells is important for the biogeochemical cycling of carbon (Berner and Honjo, 1981). The solubility of aragonite increases with depth, dropping below a saturation state of one at a depth known as the aragonite compensation depth, which is shoaling due to ocean acidification (Fabry *et al.*, 2008). Dissolution is not immediate below the aragonite compensation depth, however, and shells that sink more slowly have more time to be dissolved before reaching deeper water (Byrne *et al.*, 1984). The combination of the slower sinking rates observed here with the shoaling of the compensation depth and the elevated rate of dissolution expected from ocean acidification is likely to cause pteropod dissolution and redistribution of carbonate to occur at increasingly shallower depths.

Swimming

Although the degradation of the shell after exposure to elevated CO_2 might have been expected to have consequences to the animal's weight and ballast, swimming behaviour did not show clear changes when *L. retroversa* were exposed to elevated CO_2. In particular, unlike sinking speed, swimming speed did not show any clear reduction in the elevated CO_2 treatments. It may be that the differences among the experiments in swimming behaviour and the sensitivity of the various swimming metrics to CO_2 relate to seasonal differences in the overall condition, developmental state, and vigour of the animals prior to capture that persisted through the experiments; these differences may also be influenced by overall low sample sizes. It should also be noted that variability in individual swimming performance may have affected the patterns evident in the April and August 2014 experiments, where multiple animals were present in the filming tank concurrently, relative to the multiple runs done on individual animals in the November 2014 and April 2015 experiments. This methodological change was unfortunate and introduces the possibility of pseudoreplication in the earlier two experiments if swimming was observed for the same animal more than once. Given the overall low sample sizes and dearth of previous information, we have presented the observations from both the initial sub-optimal experiments as well as the latter two more rigorous investigations. No consistent differences across the measured swimming metrics were evident associated with the change in method.

The significant differences in swimming speed in the first week of exposure may be spurious, as the treatment with the fastest swimmers was not consistent among experiments and significant differences among treatments did not persist after longer exposure durations. A previous study by Manno *et al.* (2012) manipulated CO_2 and salinity to examine how swimming was affected in *L. retroversa* and found that elevated CO_2 alone did not cause a change in swimming speed or wing beat frequency after 8 d of exposure, while decreased salinity combined with increased CO_2 conditions slowed the swimming and increased the beat frequency. This supports the idea that our findings at 1 week are spurious.

More consistent in the present study than the patterns in swimming speed was a trend towards decreased wing beat frequency in the medium and high treatments relative to ambient, albeit only significant in one of the experiments. This reduction in wing beat frequency is interesting in its not being accompanied by an associated difference between treatments in swimming speed (although at the individual level, wing beat frequency was positively correlated with swimming speed). A reduction in beat frequency may suggest a reduced metabolic cost of swimming in the animals exposed to elevated CO_2, and is perhaps associated with a less massive shell. While there was not a good correlation between swimming speed and length, there was a significant negative correlation between wing beat frequency and length, which has also been noted in another study where larger *L. helicina* beat their wings less frequently but achieved greater speeds (Chang and Yen, 2012). That more detailed study of swimming kinetics also found that across sizes the trajectory and timing of the wing strokes varied, possibly as a response to changing Reynolds number regimes.

Tortuosity often, but not always, showed differences associated with treatment in the present study, with greatest tortuosity in the ambient treatment. Tortuosity was significantly negatively correlated to swimming speed, as animals tended to exhibit more horizontal movements that often appeared helical in nature when swimming at lower speeds. Tortuosity and length were also negatively related, though not quite significantly, whereas Chang and Yen (2012) found that the helical component of *L. helicina* swimming paths was greater for larger individuals. Pteropod swimming relies on the rotation of the shell between the power and recovery strokes and differential dissolution along the elongate shells of individual *L. retroversa* could conceivably influence swimming efficiency. Examining the asymmetry in swimming speed induced by the power and recovery strokes, however, did not show any effect of CO_2 exposure. In general, it is possible that the limited effects observed on the swimming metrics examined here in relation to CO_2 exposure are due to shell dissolution (and associated potential impacts on weight and ballast) not being advanced enough to result in discernible consequences to swimming. If future studies can overcome limitations in the durations over which pteropods can be maintained in captivity, the longer term effects on locomotion of enhanced CO_2 might be examined.

Conclusions

This study observed decreased sinking speeds in pteropods exposed to conditions of elevated CO_2 that could exist by the end of the century, suggesting that ocean acidification could affect pteropod fitness, as sinking is a mode of predator avoidance. Decreased sinking speeds will likely also slow the passive transport of calcium carbonate to depth. Ocean acidification could potentially also increase the visibility of pteropods to predators, because increased CO_2 significantly affected the transparency of shells. Longer perturbation experiments or greater replication may be needed to understand whether ocean acidification affects swimming. The cues that pteropods respond to that motivate their upward swimming are not known, and whether these cues are influenced by CO_2 treatment is also uncertain. Overall, more behavioural experiments on pteropods are needed to understand the consequences of ocean acidification, although this relies on the development of improved culture techniques in order to

achieve adequately large sample sizes and to examine impacts over longer time periods (Howes *et al.*, 2014).

Supplementary data

Supplementary material is available at the *ICESJMS* online version of the manuscript.

Acknowledgements

We would like to thank Captain K. Houtler and Mate I. Hanley of the R/V *Tioga* for their efforts that allowed us to collect the necessary number of pteropods. We appreciate the help we received at sea and in the lab collecting and rearing the pteropods from P. Alatalo, L. Blanco Bercial, S. Chu, N. Copley, T. Crockford, S. Crosby, M. Edenius, K. Hoering, R. Levine, M. Lowe, C. Pagniello, A. Schlunk, A. Tarrant, A. Thabet, T. White and P. Wiebe. We thank R. Galat and D. McCorkle for their help setting up the CO_2 exposure system and S. Chu, K. Hoering, K. Morkeski, and Z. Sandwich for their invaluable help measuring carbonate chemistry. K. Young provided much appreciated analysis code for filming. We also thank S. Colin, J. Costello, H. Jiang, and L. Mullineaux for loaning equipment used for filming. We thank C. Ashjian and two anonymous reviewers for providing helpful comments on manuscript drafts.

Funding

Funding for this research was provided by a National Science Foundation grant to GLL, AEM, and Tarrant (OCE-1316040). Additional support for field sampling was provided by the WHOI Coastal Ocean Institute, Pickman Foundation, and the Tom Haas Fund at the New Hampshire Charitable Foundation.

References

Ackman, R. G., Hingley, J., and MacKay, K. T. 1972. Dimethyl sulfide as an odor component in Nova Scotia fall mackerel. Journal of Fisheries Research Board of Canada, 29: 1085–1088.

Almogi-Labin, A., Luz, B., and Duplessy, J.-C. 1986. Quaternary paleo-oceanography, pteropod preservation and stable-isotope record of the Red Sea. Palaeogeography, Palaeoclimatology, Palaeoecology, 57: 195–211.

Armstrong, J. L., Boldt, J. L., Cross, A. D., Moss, J. H., Davis, N. D., Meyers, K. W., Walker, R. V. et al. 2005. Distribution, size, and interannual, seasonal and diel food habits of northern Gulf of Alaska juvenile pink salmon, *Oncorhynchus gorbuscha*. Deep-Sea Research II: Tropical Studies in Oceanography, 52: 247–265.

Bednaršek, N., and Ohman, M. D. 2015. Changes in pteropod distributions and shell dissolution across a frontal system in the California Current System. Marine Ecology Progress Series, 523: 93–103.

Bednaršek, N., Feely, R. A., Reum, J. C. P., Peterson, B., Menkel, J., Alin, S. R., and Hales, B. 2014. *Limacina helicina* shell dissolution as an indicator of declining habitat suitability owing to ocean acidification in the California Current Ecosystem. Proceedings of the Royal Society B, 281: 20140123.

Bednaršek, N., Tarling, G. A., Bakker, D. C., Fielding, S., Jones, E. M., Venables, H. J., Ward, P. et al. 2012. Extensive dissolution of live pteropods in the Southern Ocean. Nature Geoscience, 5: 881–885.

Berner, R. A., and Honjo, S. 1981. Pelagic sedimentation of aragonite: its geochemical significance. Science, 211: 940–942.

Busch, D. S., Maher, M., Thibodeau, P., and McElhany, P. 2014. Shell condition and survival of Puget Sound pteropods are impaired by ocean acidification conditions. PLoS One, 9: e105884.

Byrne, R. H., Acker, J. G., Betzer, P. R., Feely, R. A., and Cates, M. H. 1984. Water column dissolution of aragonite in the Pacific Ocean. Nature, 312: 322–326.

Chan, K. Y. K., Grünbaum, D., and O'Donnell, M. J. 2011. Effects of ocean acidification induced morphological changes on larval swimming and feeding. The Journal of Experimental Biology, 214: 3857–3867.

Chang, Y., and Yen, J. 2012. Swimming in the intermediate Reynolds range: kinematics of the pteropod *Limacina helicina*. Integrative and Comparative Biology, 52: 597–615.

Comeau, S., Alliouane, S., and Gattuso, J. P. 2012. Effects of ocean acidification on overwintering juvenile Arctic pteropods *Limacina helicina*. Marine Ecology Progress Series, 456: 279–284.

Comeau, S., Gorsky, G., Jeffree, R., Teyssié, J. L., and Gattuso, J. P. 2009. Key arctic pelagic mollusk (*Limacina helicina*) threatened by ocean acidification. Biogeosciences, 6: 1877–1882.

Comeau, S., Jeffree, R., Teyssié, J. L., and Gattuso, J. P. 2010. Response of the Arctic pteropod *Limacina helicina* to projected future environmental conditions. PLoS One, 5: e11362.

Conover, R. J., and Lalli, C. M. 1974. Feeding and growth in *Clione limacina* (Phipps), a pteropod mollusk. II. Assimilation, metabolism, and growth efficiency. Journal of Experimental Marine Biology and Ecology, 16: 131–154.

Dickson, A. G. 1990. Thermodynamics of the dissociation of boric acid in synthetic seawater from 273.15 to 318.15 K. Deep Sea Research, 37: 755–766.

Dickson, A. G., and Millero, F. J. 1987. A comparison of the equilibrium constants for the dissociation of carbonic acid in seawater media. Deep Sea Research, 34: 1733–1743.

Fabry, V. J., Seibel, B. A., Feely, R. A., and Orr, J. C. 2008. Impacts of ocean acidification on marine fauna and ecosystem processes. ICES Journal of Marine Science, 65: 414–432.

Gilmer, R. W., and Harbison, G. R. 1986. Structure and field behavior of pteropod molluscs: feeding methods in the families Cavoliniidae, Limacinidae, and Peraclididae (Gastropoda: Thecosomata). Marine Biology, 91: 47–57.

Haddad, G. A., and Droxler, A. W. 1996. Metastable $CaCO_3$ dissolution at intermediate water depths of the Caribbean and western North Atlantic: implications for intermediate water circulation during the past 200,000 years. Paleoceanography, 11: 701–716.

Howes, E. L., Bednaršek, N., Büdenbender, J., Comeau, S., Doubleday, A., Gallager, S. M., Hopcroft, R. R., *et al.* 2014. Sink and swim: a status review of thecosome pteropod culture techniques. Journal of Plankton Research, 36: 299–315.

Hunt, B. P. V., Pakhomov, E. A., Hosie, G. W., Siegel, V., Ward, P., and Bernard, K. 2008. Pteropods in the southern ocean ecosystems. Progress in Oceanography, 78: 193–221.

Karnovsky, N. J., Hobson, K. A., Iverson, S., and Hunt, G. L. 2008. Seasonal changes in diets of seabirds in the North Water Polynya: a multiple-indicator approach. Marine Ecology Progress Series, 357: 291–299.

Lalli, C. M., and Gilmer, R. W. 1989. Pelagic snails: the biology of holoplanktonic gastropod mollusks. Stanford University Press, Los Altos. 259 pp.

LeBrasseur, R. J. 1966. Stomach contents of salmon and steelhead trout in the Northeastern Pacific Ocean. Journal of Fisheries Research Board of Canada, 23: 85–100.

Levasseur, M., Keller, M. D., Bonneau, E., D'Amours, D., and Bellows, W. K. 1994. Oceanographic basis of a DMS-related Atlantic cod (Gadus morhua) fishery problem: blackberry feed. Canadian Journal of Fisheries and Aquatic Sciences, 51: 881–889.

Lischka, S., Büdenbender, J., Boxhammer, T., and Riebesell, U. 2011. Impact of ocean acidification and elevated temperatures on early juveniles of the polar shelled pteropod *Limacina helicina*: mortality, shell degradation, and shell growth. Biogeosciences, 8: 919–932.

Lischka, S., and Riebesell, U. 2012. Synergistic effects of ocean acidification and warming on overwintering pteropods in the Arctic. Global Change Biology, 18: 3517–3528.

Maas, A. E., Wishner, K. F., and Seibel, B. A. 2012. Metabolic suppression in thecosomatous pteropods as an effect of low temperature and hypoxia in the eastern tropical North Pacific. Marine Biology, 159: 1955–1967.

Manno, C., Morata, N., and Primicerio, R. 2012. *Limacina retroversa's* response to combined effects of ocean acidification and sea water freshening. Estuarine, Coastal and Shelf Science, 113: 163–171.

Mehrbach, C., Culberson, C. H., Hawley, J. E., and Pytkowicz, R. M. 1973. Measurement of apparent dissociation constants of carbonic acid in seawater at atmospheric pressure. Limnology and Oceanography, 18: 897–907.

Murphy, D. W., Adhikari, D., Webster, D. R., and Yen, J. 2016. Underwater flight by the planktonic sea butterfly. Journal of Experimental Biology, 219: 535–543.

Orr, J. C., Fabry, V. J., Aumont, O., Bopp, L., Doney, S. C., Feely, R. A., Gnanadesikan, A. et al. 2005. Anthropogenic ocean acidification over the twenty-first century and its impacts on calcifying organism. Nature, 437: 681–686.

Owen, J. P., and Ryu, W. S. 2015. The effects of linear and quadratic drag on falling spheres: an undergraduate laboratory. European Journal of Physics, 26: 1085–1091.

Pakhomov, E. A., Perissinotto, R., and McQuaid, C. D. 1996. Prey composition and daily rations of myctophid fishes in the Southern Ocean. Marine Ecology Progress Series, 134: 1–14.

Pierrot, D., Lewis, E., and Wallace, D. 2006. Co2sys DOS Program developed for CO2 system calculations. Carbon Dioxide Information Analysis Center, Oak Ridge National Laboratory, US Department of Energy ORNL/CDIAC-105.

Pomerleau, C., Lesage, V., Ferguson, S. H., Winkler, G., Petersen, S. D., and Higdon, J. W. 2012. Prey assemblage isotopic variability as a tool for assessing diet and the spatial distribution of bowhead whale *Balaena mysticetus* foraging in the Canadian eastern Arctic. Marine Ecology Progress Series, 469: 161–174.

Raven, J., Caldeira, K., Elderfield, H., Hoegh-Guldberg, O., Liss, P., Riebesell, U., Shepherd, J., Turley, C. and Watson, A., 2005. Ocean acidification due to increasing atmospheric carbon dioxide. Policy Document 12/05. The Royal Society, London, 60 pp.

Sabine, C. L., Feely, R. A., Gruber, N., Key, R. M., Lee, K., Bullister, J. L., Wanninkhof, R. et al. 2004. The oceanic sink for anthropogenic CO_2. Science, 305: 367–371.

Sturdevant, M. V., Orsi, J. A., and Fergusson, E. A. 2013. Diets and trophic linkages of epipelagic fish predators in coastal Southeast Alaska during a period of warm and cold climate years, 1997-2011. Marine and Coastal Fisheries: Dynamics, Management, and Ecosystem Science, 4: 526–545.

Thabet, A. A., Maas, A. E., Lawson, G. L., and Tarrant, A. M. 2015. Life cycle and early development of the thecosomatous pteropod *Limacina retroversa* in the Gulf of Maine, including the effect of elevated CO_2 levels. Marine Biology, 162: 2235–2249.

Walker, J. A. 2002. Functional morphology and virtual models: physical constraints on the design of oscillating wings, fins, legs, and feed at Intermediate Reynolds Numbers. Integrative and Comparative Biology, 42: 232–242.

Wall-Palmer, D., Smart, C. W., and Hart, M. B. 2013. In-life pteropod shell dissolution as an indicator of past ocean carbonate saturation. Quaternary Science Reviews, 81: 29–34.

Wang, Z. A., and Cai, W. J. 2004. Carbon dioxide degassing and inorganic carbon export from a marsh-dominated estuary (the Duplin River): a marsh CO_2 pump. Limnology and Oceanography, 49: 341–354.

Wang, Z. A., Wanninkhof, R., Cai, W. J., Byrne, R. H., Hu, X., Peng, T. H., and Huang, H. J. 2013. The marine inorganic carbon system along the Gulf of Mexico and Atlantic coasts of the United States: insights from transregional coastal carbon study. Limnology and Oceanography, 58: 325–342.

Wanninkhof, R., Barbero, L., Byrne, R., Cai, W. J., Huang, W. J., Zhang, J. Z., Baringer, M., and Langdon, C. 2015. Ocean acidification along the Gulf Coast and East Coast of the USA. Continental Shelf Resesarch, 98: 54–71.

Wheeler, J. D., Helfrich, K. R., Anderson, E. J., McGann, B., Staats, P., Wargula, A. E., Wilt, K., and Mullineaux, L. S. 2013. Upward swimming of competent oyster larvae *Crassostrea virginica* persists in highly turbulent flow as detected by PIV flow subtraction. Marine Ecology Progress Series, 488: 171–185.

Wormuth, J. H. 1981. Vertical distributions and diel migrations of *Euthecosomata* in the northwest Sargasso Sea. Deep-Sea Research, 28A: 1493–1515.

Handling editor: David M. Fields